JOURNAL OF MATERIALS SCIENCE 36 (2001) 3997–4002

A TEM investigation of Zn_3As_2 grown on (001) and (111) InP by MOVPE

J. H. NEETHLING*, G. J. SCRIVEN
Department of Physics, University of Port Elizabeth, P.O. Box 1600, Port Elizabeth, 6000, South Africa
E-mail: phajhn@upe.ac.za

T. KREKELS
Philips Electron Optics, Eindhoven, The Netherlands

A TEM investigation of MOVPE grown Zn_3As_2 revealed the presence of a thin epitaxial Zn_3P_2 intermediate layer between the InP substrate and the Zn_3As_2 overgrowth. A model of the orientation relationships between Zn_3As_2, Zn_3P_2 and InP is presented. The origin of the Zn_3P_2 layer was ascribed to the diffusion of Zn atoms into the InP substrate, aided simultaneously by P diffusion from the substrate. A simulation of the Zn_3As_2 lattice image is presented for the first time, together with a high resolution transmission electron microscopy (HRTEM) image of the Zn_3As_2/Zn_3P_2 interface.

1. Introduction

Zn_3As_2 belongs to the II_3-V_2 group of semiconductors which has not been as widely investigated as the III-V and II-VI semiconducting materials. Zn_3As_2 forms one binary end-point of the ternary semiconductors $Zn_xCd_{3-x}As_2$ [1]. These compounds are characterized by an energy gap tunable from −0.19 eV to 0.99 eV as x is varied from 0 to 3. This makes $Zn_xCd_{3-x}As_2$ attractive for long wavelength photonic devices and an alternative to $Cd_yHg_{1-y}Te$ as an infrared detecting material since the difference between the energy gaps of the binary end-points of $Cd_yHg_{1-y}Te$ is significantly larger than is the case for $Zn_xCd_{3-x}As_2$. Therefore, a small variation in composition as a result of crystal growth will have a much smaller effect on the cut-off wavelength in the case of $Zn_xCd_{3-x}As_2$ than for $Cd_yHg_{1-y}Te$. One of the biggest problems associated with $Zn_xCd_{3-x}As_2$ is that undoped Zn_3As_2 was, until the present, always found to be p-type, with hole concentrations in the order of mid 10^{17}–10^{18} cm^{-3}. Material with lower hole concentrations, obtained by doping with Se [2], necessarily lead to compensated material. Recently, however, undoped Zn_3As_2 crystals with hole concentrations as low as 3.3×10^{16} cm^{-3} were prepared by making use of (metalorganic vapour phase epitaxy) MOVPE [3].

The II_3-V_2 materials all have extremely complicated crystal structures and large unit cells. Zn_3As_2 crystallises in a body-centred tetragonal structure consisting of 16 defect fluorite (CaF_2) cells with 64 close packed As and 96 Zn atoms distributed among 128 tetrahedral voids in the unit cell [4, 5]. This large unit cell (see Fig. 1) contains 512 valence electrons [6]. The commonality of the anion sublattice makes the II_3-V_2 materials more compatible for growth on III-V substrates such as GaAs and InP than is the case for II-VI materials [7]. The lattice parameters of Zn_3As_2 are $a = b = 1.17786$ nm and $c = 2.36432$ nm (resulting in c/a ratio of 2.007) and reveals an excellent lattice match to InP since $a = b = 1.00355 \times 2a_{InP}$ and $c = 1.0072 \times 4a_{InP}$ [8].

It was shown in a previous report [9] that (001) Zn_3As_2 grows parallel to (001) InP, for growth on (001) oriented InP, while (112) Zn_3As_2 grows parallel to (111) InP, for growth on (111) oriented InP by MOVPE. Cross-sectional scanning electron microscope micrographs showed the interfaces between the epilayers and the substrate clearly, and it appeared that Zn_3As_2 grew epitaxially on InP. Recent transmission electron microscope (TEM) analysis of these interfaces, however, revealed the presence of an intermediate layer between the epitaxial Zn_3As_2 layer and the InP substrate. The aim of this present study is therefore to identify the nature and origin of this intermediate layer. The Zn_3As_2 unit cell is also modeled and a HRTEM image thereof is simulated using the EMS 3.3 software [10].

2. Experimental

Single crystalline Zn_3As_2 epitaxial layers were grown by MOVPE in a horizontal Thomas Swan reactor under atmospheric pressure. DEZn and AsH_3 (10 vol% diluted in H_2) were used as the group II and V precursors, respectively. The growth temperature was 450 °C for all layers involved while ultraviolet light was used to precrack the arsine at the reactor entrance. A Zn

*Author to whom all correspondence should be addressed.

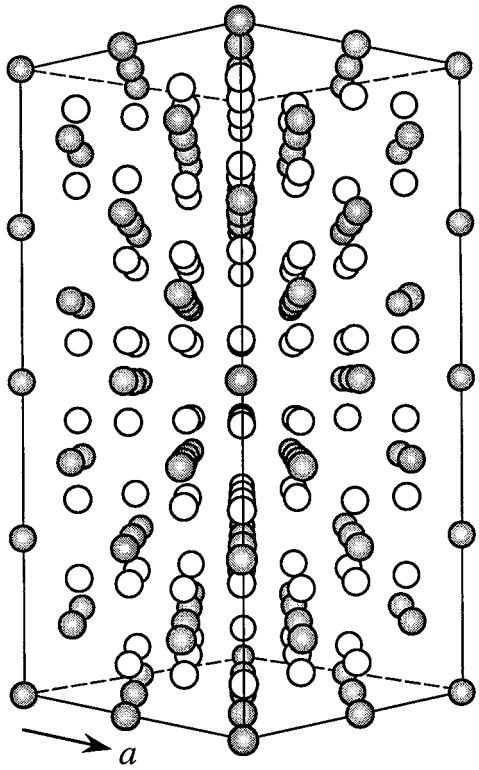

Figure 1 The unit cell of Zn_3As_2 as viewed along the [110] direction. Shaded spheres denote As atoms while Zn atoms are denoted by white spheres.

mole fraction of 7.4×10^{-5} was employed while the As mole fraction was kept constant, resulting in a V/II ratio of 44 for all layers involved in the study. Palladium diffused hydrogen was used as a carrier gas at a flow rate of 2 l/min. Layers were grown on semi-insulating (Fe doped) oriented 2° off the (001) plane InP and Ge doped (111) oriented InP. The layers under investigation had thicknesses of approximately 1.5 μm. TEM specimens were prepared by using standard thinning and milling techniques.

A Philips XL30 scanning electron microscope and Philips EM420 transmission electron microscope (TEM), the latter equipped with a LaB_6 filament, were used to examine the Zn_3As_2 epilayers. The TEM is also equipped with an EDAX energy dispersive X-ray spectrometer with a super ultra thin window detector, that was used to determine the composition of the epitaxially grown material. High resolution TEM was performed on a 200 kV Philips CM 200 FEG (super twin).

3. Results

Fig. 2 is a cross-sectional scanning electron microscope (SEM) micrograph of a Zn_3As_2 epilayer grown on (001) oriented InP. It can be clearly seen that the surface exhibits preferred crystallographic features which terminate on {224} planes. These {224} planes make an angle of 54.7° with the (001) substrate. The prominence of the {224} planes, rather than other planes, indicates that the former most probably have a higher surface energy. The (224) plane of Zn_3As_2 is the most densely packed plane and, therefore, dislocation glide is expected to occur on the {224} planes.

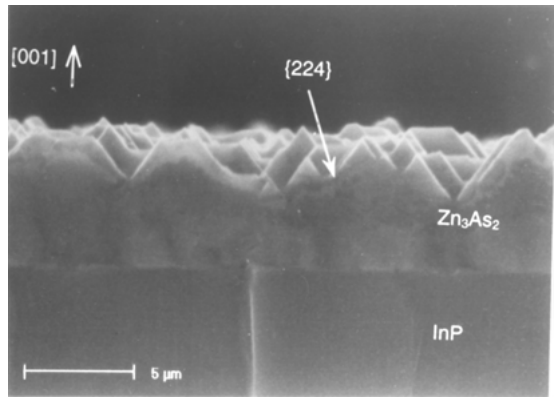

Figure 2 Cross-sectional SEM image of a Zn_3As_2 epilayer grown on (001) InP.

Fig. 3a shows a TEM micrograph of the interfacial area of a Zn_3As_2 epilayer grown on (001) oriented InP. An intermediate layer, sandwiched between the Zn_3As_2 and the InP substrate can be seen clearly. Energy dispersive X-ray spectrometry (EDS) was used to determine the composition of each individual layer visible in the micrograph and the results are plotted in Fig. 3b. The atomic concentrations of all the elements, except the Cu (which arises from the grid that supports the sample), present in the EDS spectra are also shown in Fig. 3b.

The intermediate layer is also detected when growth of Zn_3As_2 is performed on (111) oriented InP. Results of EDS analysis for a Zn_3As_2 epilayer grown on this substrate orientation are presented in Table I. It can be seen that the concentration of each element in the various layers is approximately the same for growth on both substrate orientations.

It can be seen that the Zn:As atomic concentration in the epilayer is approximately 3:2, which is consistent with the earlier identification of this layer by X-ray diffraction [8] as Zn_3As_2. The In:P concentration ratio in the substrate was found to be 1 : 0.75, indicating that out-diffusion of P had taken place during the growth process. The InP substrate has therefore provided the phosphorus for the formation of the intermediate layer. The electron probe diameter used for the EDS analysis was of the same magnitude as the thickness of the intermediate layer and therefore the EDS spectrum of this layer also contains contributions from the Zn_3As_2 epilayer and the InP substrate. Substracting the estimated contributions from the EDS spectra of P belonging to the substrate and Zn belonging to the epilayer yielded a Zn:P ratio of approximately 3:2. This is consistent with the identification of the intermediate layer as the group II_3-V_2 semiconductor Zn_3P_2.

TABLE I Results of EDS analysis for a Zn_3As_2 epilayer grown on (111) InP

Zn_3As_2 epitaxial layer		Intermediate layer		InP substrate	
Element	Atomic %	Element	Atomic %	Element	Atomic %
In	0	In	13	In	57
P	0	P	38	P	43
Zn	62	Zn	47	Zn	0
As	38	As	2	As	0

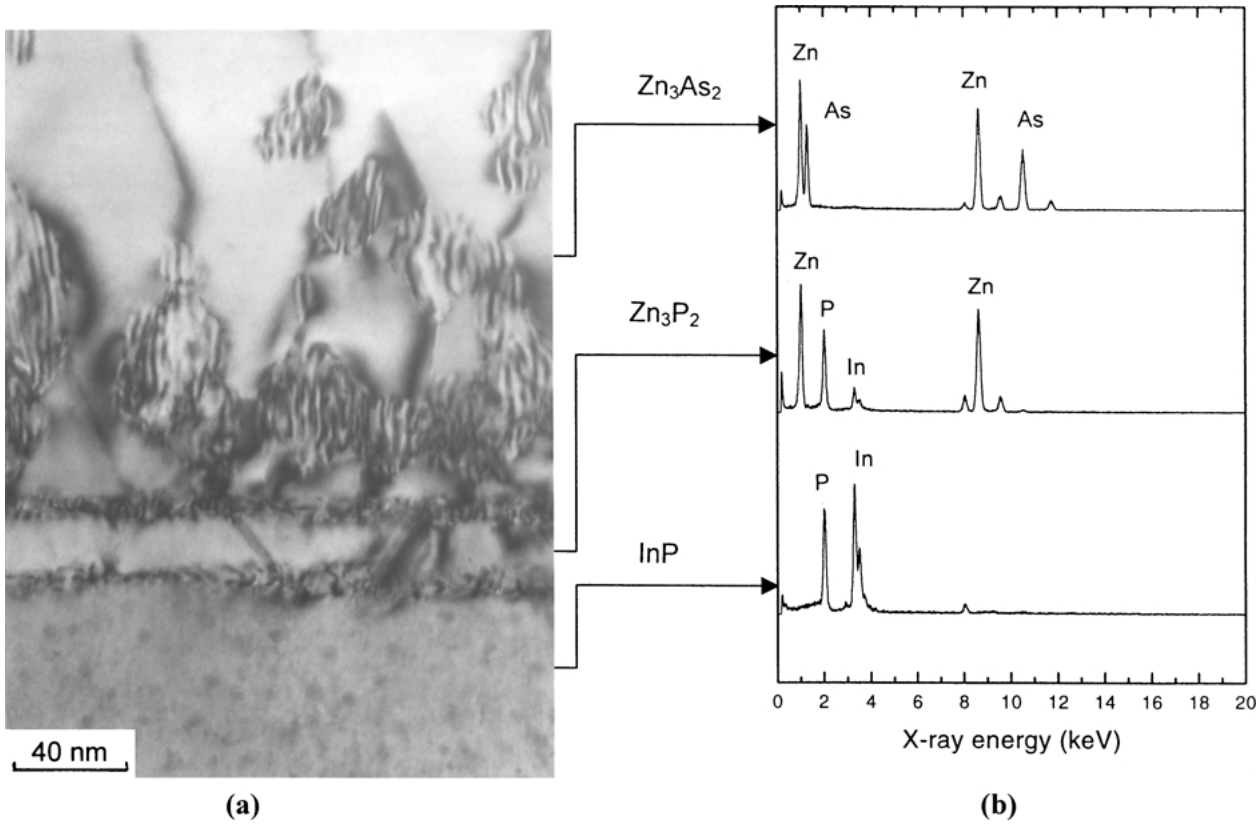

Figure 3 (a) Cross-sectional TEM image of a Zn_3As_2 epilayer grown on (001) InP and (b) Energy dispersive X-ray spectra for the InP substrate, the intermediate layer, and the Zn_3As_2 epilayer.

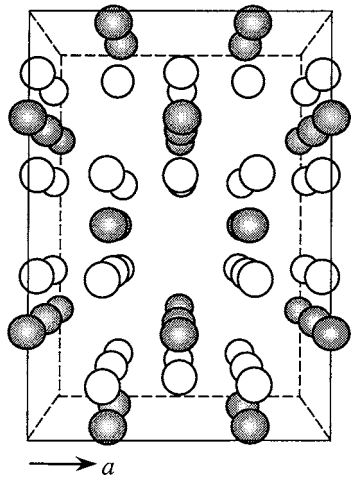

Figure 4 The unit cell of Zn_3P_2 as viewed along the [100] direction. Shaded spheres denote P atoms while Zn atoms are denoted by white spheres.

Zn_3P_2 crystallizes in a primitive tetragonal structure, with a unit cell consisting of 16 P atoms and 24 Zn atoms [11]. A schematic illustration of its unit cell, viewed along the [100] direction, is shown in Fig. 4. The Zn atoms are located on four equally spaced planes perpendicular to the c-axis, while the P atoms lie on parallel planes midway between two Zn planes. Each Zn atom is tetrahedrally coordinated with P atoms as their nearest neighbours, while a P atom is surrounded by Zn atoms located at six of the eight corners of a cube, the two vacant sites being at diagonally opposite corners of a cubic face [11]. The space group of Zn_3P_2 belongs to P4/nmc [12]. The lattice parameters of Zn_3P_2 are $a = b = 0.8113$ nm, $c = 1.147$ nm, with $c/a = 1.41$ [6].

Fig. 5a shows the selected area diffraction (SAD) patterns of the InP substrate and the Zn_3As_2 layer of the sample of which the TEM micrograph is shown in Fig. 3a. The beam direction is [110]. The patterns are characteristic of materials with the crystal structures of InP and Zn_3As_2. The pattern that is observed for Zn_3As_2 is identical to that obtained by Chelluri *et al.* [1] for a Zn_3As_2 sample grown on InP by MBE, viewed along the same direction. As is expected, identical results are also obtained when Zn_3As_2 is grown on (111) InP. The SAD pattern of the Zn_3As_2 epilayer was indexed by making use of the InP SAD pattern to calibrate the camera constant. The indices of some reflections are shown in Fig. 5a. Analysis of the matrix and epilayer spots revealed the following orientation relationships between the substrate and epilayer:

$$(001)\mathrm{InP} \parallel (001)\mathrm{Zn_3As_2} \text{ and } [\bar{1}10]\mathrm{InP} \parallel [\bar{1}10]\mathrm{Zn_3As_2}.$$

The former relationship is consistent with the findings of X-ray diffraction [9].

Micro-diffraction that was performed on the same sample (shown in Fig. 5b) gives rise to almost identical patterns as the beam was moved from the InP substrate to the intermediate layer. It can be seen from the figure that all the major reflections overlap. Similar results are obtained for growth on (111) oriented InP. This is a surprising result since the crystal structure and the lattice parameters of Zn_3P_2 and InP are different. However,

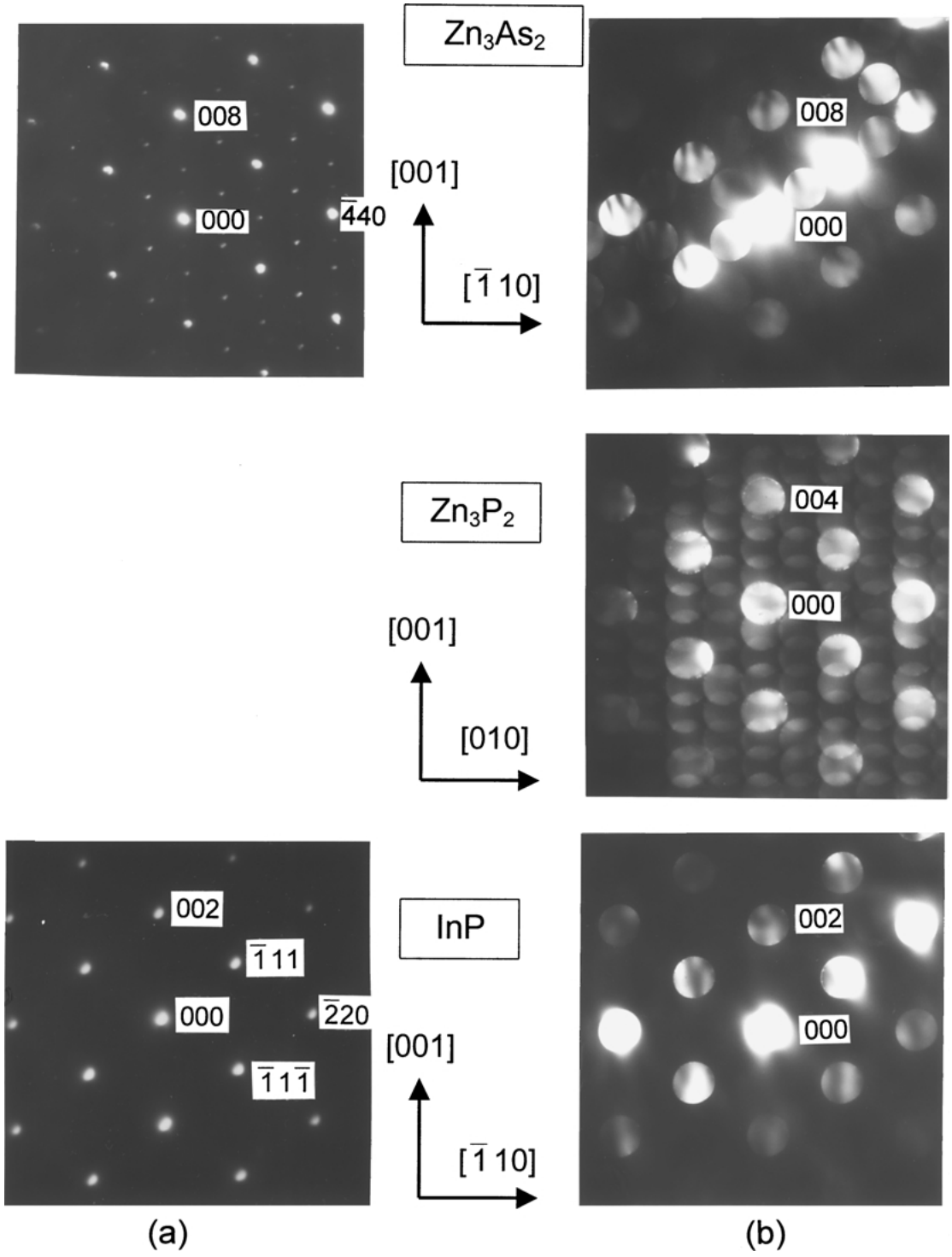

Figure 5 (a) SAD patterns of Zn_3As_2 and InP for growth on (001) oriented InP. (b) Micro-diffraction patterns of the Zn_3As_2 epilayer, the Zn_3P_2 intermediate layer and the substrate for the same layer. The beam directions are [110] for Zn_3As_2 and InP, while it is [100] for the Zn_3P_2 intermediate layer.

when Zn_3P_2 and InP are viewed along the respective [100] and [110] directions almost identical diffraction patterns are generated. Table II lists the interplanar distances for some of the planes of which the reflections in Fig. 5b overlap. The micro-diffraction patterns thus indicate that Zn_3P_2 and InP have the following orientation relationship:

$$(001)\text{InP} \parallel (001)Zn_3P_2 \text{ and } [\bar{1}10]\text{InP} \parallel [010]Zn_3P_2.$$

Using the orientation relationships deduced by SAD and microdiffraction, a schematic representation of the growth of Zn_3P_2 on (001) oriented InP, with the subsequent overgrowth of Zn_3As_2 on Zn_3P_2, is shown in Fig. 6. The shaded areas denote the planes that will be parallel to the surface of substrate, when Zn_3As_2 is grown on (111) oriented InP.

An explanation for the formation of the Zn_3P_2 layer may be found in a paper published by Hwang *et al*. [13] in which it is described how $InP/In_{0.53}Ga_{0.47}As$ superlattices can be converted into $Zn_3P_2/In_{1-x}Ga_xAs$ and Zn_3P_2/Zn_3As_2 superlattices by making use of Zn diffusion. The authors subjected unstrained $InP/In_{0.53}Ga_{0.47}As$ superlattices to

TABLE II Interplanar distances for Zn_3P_2 and InP overlapping reflections

InP (hkl)	d (nm)	Zn_3P_2 (hkl)	d (nm)
002	0.294	004	0.285
111	0.339	022	0.329
220	0.208	040	0.201

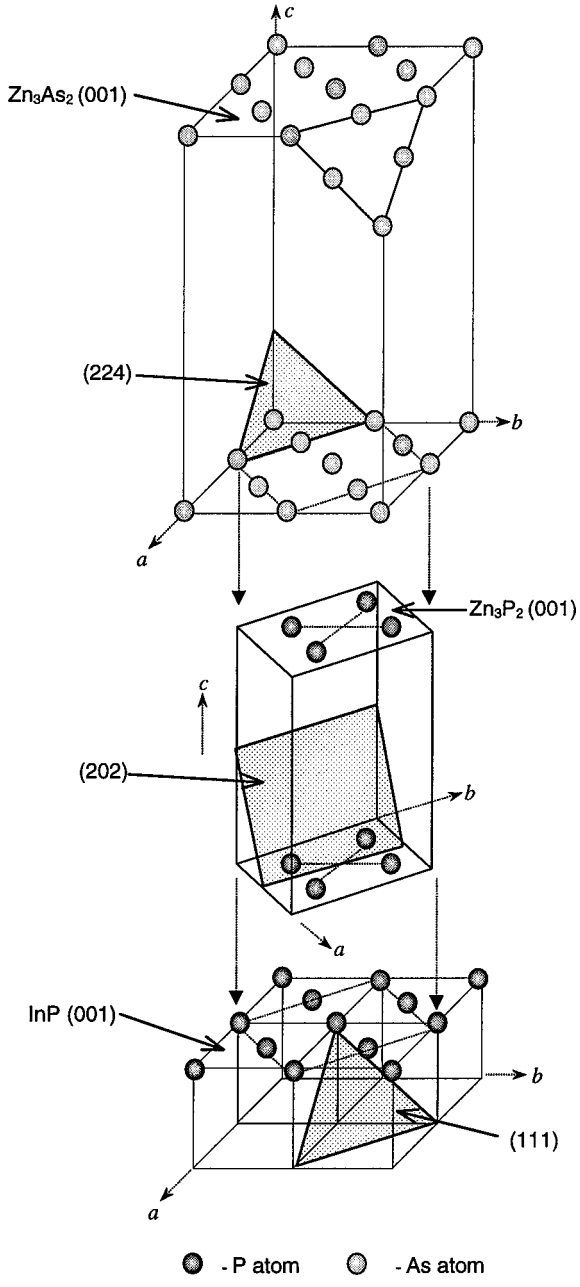

Figure 6 Schematic illustration of the orientation relationships of Zn_3As_2 grown on (001) oriented InP. The shaded areas denote the {224}, {202} and {111} planes of Zn_3As_2, Zn_3P_2 and InP, respectively. These planes will be parallel to the surface when growth is performed on (111) oriented InP.

Zn diffusion in evacuated sealed quartz tubes with a Zn_3As_2 powder source at 600 °C. The authors found that continued infusion of Zn resulted in the total replacement of In and Ga with Zn, progressively from the surface, and selectively from the P layers first, then from the As layers. The authors surmised that the In and Ga atoms that were replaced by Zn atoms eventually escaped from the surface. They further reported that no diffusion of P and As was observed.

From the results of Hwang *et al*. [13] it is clear that Zn has a lower binding energy with P than it has with As, and it is likely that a similar phenomenon to that which has been described by Hwang *et al*. has occurred with the MOVPE grown Zn_3As_2 epilayers in this study. At the instant that Zn is injected into the reactor, Zn diffusion into InP appears to be occurring, in spite of the fact that the growth temperature of 450 °C is much lower than was the case in the experiment of Hwang *et al*. It is likely that In atoms are therefore replaced by Zn atoms, from the surface, at first, but then progressively deeper into the InP substrate material. It is believed that the In atoms that are replaced by the Zn atoms escape from the substrate surface, as was described by Hwang *et al*. [13]. It is likely that the formation of Zn_3P_2 is further enhanced by the simultaneous out-diffusion of phosphorous from the InP substrate. This process will, however, compete with As to form Zn_3As_2. It is suggested that after the Zn_3P_2 intermediate layer has reached a certain thickness, it will be more favorable for Zn_3As_2 to form than Zn_3P_2, and from this point onwards the growth of Zn_3As_2 on Zn_3P_2 will dominate.

It would be difficult to stop the intermediate layer from forming, since the diffusion of the Zn atoms is likely to be thermally driven. This would explain why no Zn_3P_2 layer appeared in the MBE grown Zn_3As_2 by Chelluri *et al*. [1] since their growth temperature was 360 °C, which is significantly lower than the growth temperature that was used in this study for the MOVPE grown epilayers. This would suggest that the growth temperature for the MOVPE grown layers should be lowered to prevent the formation of the intermediate layer. However, growth of Zn_3As_2 by MOVPE using lower temperatures leads to polycrystalline epilayers [9].

Fig. 7 shows a high resolution TEM micrograph of the interface region between the Zn_3As_2 epilayer and the intermediate layer grown at 450 °C on (001) InP. The electron beam direction is [110] and [100] with respect to Zn_3As_2 epilayer and the Zn_3P_2 intermediate layer, respectively.

It can be shown that the {224} plane of Zn_3As_2 and the {202} plane of Zn_3P_2 make an angle of 54.8° and 54.7° with their {001} planes, respectively, while the angle between the {111} and {001} planes of InP is 54.7°. As expected, the TEM lattice image shows the {224} Zn_3As_2 and {202} Zn_3P_2 planes making an angle of approximately 55° with the (001) interface. The interface between the Zn_3As_2 and the Zn_3P_2 intermediate layer is indicated on the micrograph. Due to the small difference in interplanar spacing between the {202} planes of Zn_3P_2 ($d_{022} = 3.29$ Å) and the {224} planes of Zn_3As_2 ($d_{\{224\}} = 3.40$ Å), the {202} planes of Zn_3P_2 appear to be continuous across the interface, where they become the {224} planes in Zn_3As_2.

It is expected that the lattice images of the Zn_3As_2 and Zn_3P_2 will be nearly identical, since their SAD patterns are nearly identical for the respective beam directions along which the two materials are viewed.

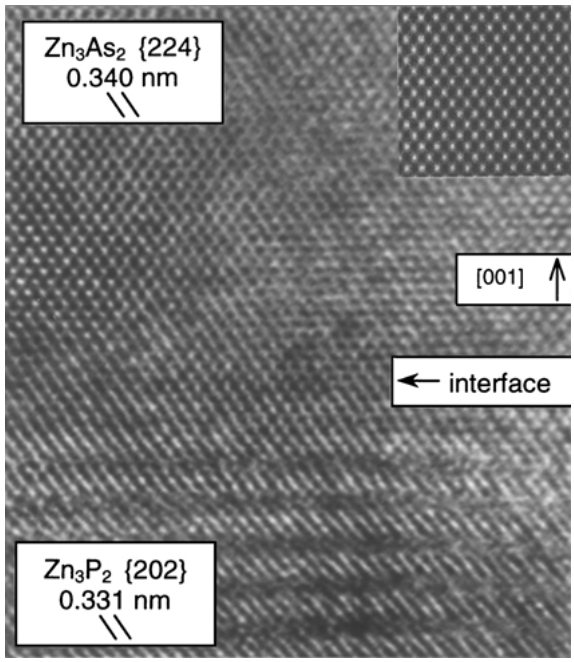

Figure 7 Cross-sectional HR TEM micrographs showing the interface between the Zn_3As_2 epilayer and the intermediate layer for growth at 450 °C on (001) oriented InP. The electron beam direction is [110] with respect to the Zn_3As_2 and [100] with respect to Zn_3P_2. The inset is a simulated HRTEM lattice image of Zn_3As_2.

The fact that the Zn_3P_2 lattice image differ from the Zn_3As_2 lattice image in the micrograph shown in Fig. 7, is ascribed to bending of the thin Zn_3P_2 foil under the electron beam, causing the beam direction in the Zn_3P_2 to be slightly off the [100] direction. The TEM lattice image also is consistent with the orientation relationship between Zn_3As_2 and Zn_3P_2 that was deduced from micro-diffraction. The inset in Fig. 7 is a simulated lattice image of the Zn_3As_2 epilayer, generated by using the EMS 3.3 [10] software package. A close agreement exists between the simulated and experimental images of Zn_3As_2.

4. Conclusions

TEM investigations of the MOVPE grown Zn_3As_2 revealed the presence of a thin intermediate layer that grew epitaxially between the InP and the Zn_3As_2 overgrowth. The layer was identified to be Zn_3P_2 by making use of EDS analysis. Micro-diffraction revealed the following orientation relationship between InP and Zn_3P_2: (001)InP ‖ (001)Zn_3P_2 and [$\bar{1}$10] InP ‖ [010]Zn_3P_2. For this orientation the lattice mismatch between Zn_3P_2 and InP is minimized. The Zn_3P_2 layer is orientated w.r.t. the Zn_3As_2 epitaxial layer in exactly the same way, so that (001) and [$\bar{1}$10] Zn_3As_2 grows parallel to (001) and [$\bar{1}$10] InP, respectively, as was indicated by SAD. The origin of the Zn_3P_2 layer was ascribed due to the diffusion of Zn atoms into the InP substrate, and the subsequent bonding of Zn with P. It is believed that P diffusion from the InP substrate contributes to the formation of Zn_3P_2. It is suggested that interstitial In atoms escape from the substrate surface. High resolution transmission electron microscopy revealed that {224} planes of Zn_3As_2 appear to be continuous across the interface, where they become the {022} planes in Zn_3P_2 for growth on (001) oriented InP. This confirms the orientation relationships that were inferred from microdiffraction. Excellent agreement was found between simulated HRTEM images and those that were obtained experimentally.

Acknowledgements

The National Research Foundation is acknowledged for their financial assistance in this project.

References

1. B. CHELLURI, T. Y. CHANG, A. OURMAZD, A. H. DAYEM, J. L. ZYSKIND and A. SRIVASTAVA, *J. Cryst. Growth* **81** (1987) 530.
2. W. J. TURNER, A. S. FISCHLER and W. E. REESE, *Physical Review* **121** (1961) 759.
3. G. J. SCRIVEN and A. W. R. LEITCH, *Thin Solid Films*, 2001, submitted.
4. B. SUJAK-CYRUL, B. KOLODKA and J. MISIEWICZ, *J. Phys. Chem. Solids* **43** (1982) 1045.
5. A. HUPFER, D. HIRSCH and S. SCHULZE, *Phys. Stat. Sol. (b)* **152** (1989) 505.
6. K. SIERAÑSKI and J. SZATKOWSKI, *ibid.* **173** (1992) K25.
7. B. CHELLURI, T. Y. CHANG, A. OURMAZD, A. H. DAYEM, J. L. ZYSKIND and A. SRIVASTAVA, *Appl. Phys. Lett.* **49** (1986) 1665.
8. A. PIETRASZKO and K. LUKASZEWICZ, *Phys. Stat. Sol. (a)* **18** (1973) 723.
9. G. J. SCRIVEN, A. W. R. LEITCH, J. H. NEETHLING, V. V. KOZYRKOV and V. J. WATTERS, *J. Cryst. Growth* **170** (1997) 813.
10. P. STADELMAN, EMS 3.3., *Ultramicroscopy* **21** (1987) 131.
11. K. SIERAÑSKI, J. SZATKOWSKI and J. MISIEWICZ, *Physical Review B* **50** (1994) 7331.
12. R. W. G. WYCKOFF, "Crystal Structures: Volume 2, Inorganic Compounds RX_n, R_nMX_2, R_nMX_3" (Interscience Publishers, New York, 1964) p. 32.
13. D. M. HWANG, S. A. SCHWARZ, P. MEI, R. BHAT, T. VENKATESAN, L. NAZAR and C. L. SCHWARZ, *Appl. Phys. Lett.* **54** (1989) 1160.

Received 10 November
and accepted 14 December 1999